

**TECTONIC UPLIFTS BASED ON
MORPHOMETRIC INDICES IN NORTH WEST
SABAH, MALAYSIA**

CHUNG WEI KIAT



UMS

**THESIS SUBMITTED IN FULFILLMENT FOR THE
DEGREE OF DOCTOR OF PHILOSOPHY**

**FACULTY OF SCIENCE AND NATURAL
RESOURCES
UNIVERSITI MALAYSIA SABAH
2020**

UNIVERSITI MALAYSIA SABAH

BORANG PENGESAHAN STATUS TESIS

JUDUL : **TECTONIC UPLIFTS BASED ON MORPHOMETRIC INDICES IN NORTH WEST SABAH, MALAYSIA**

IJAZAH : **DOKTOR FALSAFAH**

BIDANG : **GEOLOGI**

Saya **CHUNG WEI KIAT**, Sesi **2018-2020**, mengaku membenarkan tesis Doktoral ini disimpan di Perpustakaan Universiti Malaysia Sabah dengan syarat-syarat kegunaan seperti berikut:-

1. Tesis ini adalah hak milik Universiti Malaysia Sabah
2. Perpustakaan Universiti Malaysia Sabah dibenarkan membuat salinan untuk tujuan pengajian sahaja.
3. Perpustakaan dibenarkan membuat salinan tesis ini sebagai bahan pertukaran antara institusi pengajian tinggi.
4. Sila tandakan (/):

SULIT

(Mengandungi maklumat yang berdarjah keselamatan atau kepentingan Malaysia seperti yang termaktub di dalam AKTA RAHSIA 1972)

TERHAD

(Mengandungi maklumat TERHAD yang telah ditentukan oleh organisasi/badan di mana penyelidikan dijalankan)

TIDAK TERHAD

Disahkan Oleh,

CHUNG WEI KIAT
DS1721010T

(Tandatangan Pustakawan)

Tarikh : 31 October 2020

(Prof. Dr. Felix Tongkul)
Penyelia

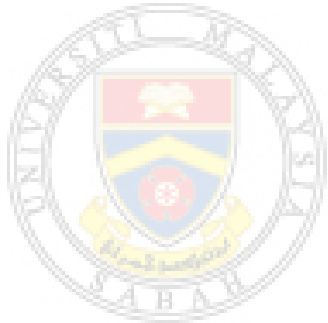
DECLARATION

I hereby declare that all results and discussion in this thesis is my own original work, while acknowledging previous works in existing literature.

4 August 2020

CHUNG WEI KIAT

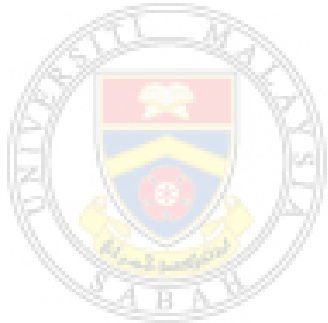
DS1721010T



UMMS
UNIVERSITI MALAYSIA SABAH

CERTIFICATION

NAME : **CHUNG WEI KIAT**
MATRIC NO : **DS1721010T**
TITLE : **TECTONIC UPLIFTS BASED ON MORPHOMETRIC INDICES IN
NORTH WEST SABAH, MALAYSIA**
DEGREE : **DOCTOR OF PHILOSOPHY**
FIELD : **GEOLOGY**
VIVA DATE : **4 AUGUST 2020**



CERTIFIED BY;
UMS
UNIVERSITI MALAYSIA SABAH
Signature

SUPERVISOR

Professor Dr. Felix Tongkul

ACKNOWLEDGEMENT

First and foremost, I would like to thank NDRC, FSSA and UMS for providing space and facilities during my doctoral studies.

Secondly, I am grateful to Professor Dr. Felix Tongkul for his guidance and time in guiding this doctoral thesis work.

I would like to thank the academic staff of Geology for their encouragement and comments in this work.

I would also like to express thanks to Mr. Kenneth Chung for his field assistance and support in taking the high-quality drone images.

Also, I would like to express thanks to fellow students in Universiti Malaysia Sabah for their friendship and support.

Last but not least, to my parents for the financial support in undertaking this doctoral study in Universiti Malaysia Sabah.

Chung Wei Kiat

4 August 2020

ABSTRACT

The study constitutes the identification of uplift sites based on gradient and erosion anomalies over four major catchments in northwest Sabah, namely Kota Belud, Tuaran, Kinabalu Northeast, and Kinabalu Southeast catchments. The objectives of the study are to identify and screen regional sites of tectonic uplifts; identify and characterize sites of local uplift; validate the tectonic uplift in the field; and infer the active tectonics of northwest Sabah. The sites of tectonic uplifts at a regional and local scale were identified using gradient and erosion metrics over the 30 m resolution SRTM digital elevation models (DEM) and 5 m resolution IFSAR digital elevation models (DTM & DSM), respectively. The gradient metrics includes stream-length gradient index, surface-shape length gradient index, and knickpoint identifications whereas the erosion metrics includes normalized channel steepness index, chi-factor analysis and minimum bulk erosion. Based on the morphometric indices, several sites located both in the western and eastern flank catchments showed significant anomalies interpreted to be uplifted sites due to faults or lithological differences. Some of the anomalies are aligned N40E and may indicate alignment of regional faults. A closer analysis of some of the most significant anomalies in 18 sites clearly showed the presence of uplifted landforms. Out of 18 uplifted sites validated and characterized in the field, 11 sites from the western flank catchments indicates a NW-SE extensional regime, where the landform appears to be stretched forming a series of rapids and small waterfalls, whereas 7 sites from the eastern flank catchments indicates a NW-SE compressional regime, where the landform appears to have buckled causing stream ponding and incised valleys. The presence of both compressional and extensional tectonic regimes in northwest Sabah may be associated with NW-SE intraplate compression and gravity sliding towards the South China Sea.

ABSTRAK

PENGANGKATAN TEKTONIK BERDASARKAN INDEKS MORPHOMETRI DI KAWASAN BARATLAUT SABAH, MALAYSIA

Kajian ini bertujuan mengenalpasti tapak terangkat berdasarkan anomali kecerunan dan hakisan di empat tadahan utama di Baratlaut Sabah, iaitu tadahan air Kota Belud, Tuaran, Timurlaut Kinabalu dan Tenggara Kinabalu. Objektif kajian adalah untuk mengenalpasti dan menyaring tapak terangkat rantau; mengenalpasti dan mencirikan tapak terangkat tempatan; mengesahkan pengangkatan tektonik di lapangan; dan mentafsir tektonik aktif di Baratlaut Sabah. Tapak terangkat pada skala rantau dan skala tempatan dikenalpasti menggunakan morfometri kecerunan dan hakisan keatas model ketinggian digital (DEM) SRTM dengan resolusi 30 m dan model ketinggian digital (DTM & DSM) IFSAR dengan resolusi 5 m. Morfometri kecerunan merangkumi indeks kecerunan panjang sungai, indeks kecerunan panjang dan bentuk permukaan, dan mengenalpastian titik perubahan kecerunan mendadak, sementara morfometri hakisan merangkumi indeks kecuraman tebing sungai, analisis faktor-chi dan hakisan pukal minimum. Berdasarkan kepada indeks morfometri, beberapa tapak yang terdapat di tadahan air di bahagian barat dan bahagian timur menunjukkan anomali yang signifikan, yang ditafsirkan sebagai tapak terangkat disebabkan oleh sesar atau perbezaan litologi. Terdapat anomali yang tersusun pada arah N40E yang mungkin mewakili orientasi sesar rantau. Analisis lebih dekat terhadap beberapa anomali yang paling signifikan di 18 tapak jelas menunjukkan kehadiran mukabumi terangkat. Dari pada 18 tapak terangkat yang disahkan dan dicirikan di lapangan, 11 tapak dari tadahan sungai bahagian barat menunjukkan regim regangan Baratlaut-Tenggara, dimana mukabumi kelihatan tertarik membentuk beberapa siri jeram dan air terjun kecil, sementara 7 tapak dari tadahan sungai di bahagian timur menunjukkan regim mampatan Baratlaut-Tenggara, dimana mukabumi kelihatan terangkat menyebabkan pembentukan kolam pada sungai dan lembah terhakis dalam. Kehadiran kedua-dua regim tektonik mampatan dan regangan di Baratlaut Sabah mungkin dikaitkan dengan mampatan Baratlaut-Tenggara plet intra dan gelinciran graviti kearah Laut China Selatan.

LIST OF CONTENTS

	Page
TITLE	i
DECLARATION	ii
CERTIFICATION	iii
ACKNOWLEDGEMENT	iv
ABSTRACT	v
<i>ABSTRAK</i>	vi
LIST OF CONTENTS	vii
LIST OF FIGURES	xi
CHAPTER 1: INTRODUCTION	1
1.1 Research Background	1
1.2 Study Location	4
1.2.1 Regional Climate	4
1.2.2 General Geology and Tectonic Setting	5
1.3 Research Problem	7
1.4 Research Objectives	8
1.5 Significance of Research	8
1.6 Scope of Study	9
1.7 Study Approach	9
CHAPTER 2: LITERATURE REVIEW	10
2.1 Introduction	10
2.2 South China Sea	11
2.2.1 The Tectonic Setting of the Proto-South China Sea to the Cenozoic Uplift of NW Sabah	11
2.2.2 The Subduction Timing of the Proto-South China Sea in Relation to the NW Borneo Uplift	13

2.2.3	Cenozoic Southeast Asia Evolution in Relation to NW Borneo Uplift	17
2.3	Regional Geology of NW Sabah	20
2.3.1	Overview	20
2.3.2	NW Sabah Tectonic Setting	21
2.3.3	NW Sabah Stratigraphy	23
2.4	Mount Kinabalu	25
2.4.1	General Geology	25
2.4.2	Tectonic Setting of the Mount Kinabalu	27
2.5	Neotectonics of NW Sabah	30
2.5.1	Overview	30
2.5.2	Compression Tectonics	30
2.5.3	Extensional Tectonics	32
2.5.4	Tectonic Imprints	32
CHAPTER 3: MATERIALS & METHODOLOGY		35
3.1	Introduction	35
3.2	Flow Chart & Study Approach	35
3.3	Materials	37
3.4	Methods	39
3.4.1	Stream-Length Gradient (Hack's and surface- shape length)	39
3.4.2	Topographic Relief Analysis	41
3.4.3	Normalised Channel Steepness Index	42
3.4.4	χ factor	43
3.4.5	Minimum Bulk Erosion, <i>E_{bulk}</i>	45
3.4.6	Hypsometric Integral	46
3.4.7	Getis-Ord (G_i^*) spatial autocorrelation	46

CHAPTER 4: MORPHOMETRIC RESULTS	47
4.1 Introduction	47
4.2 Stream-Length Gradient Index (SLGI) at 1 km Interval	48
4.3 Stream-Length Gradient Index at 100 m Interval	54
4.4 K_{sn} Anomalies Map	57
4.5 Chi Composite Map	58
4.6 Hypsometric Integral, HI Composite Map	60
4.7 Minimum Bulk Erosion, <i>E_{bulk}</i>	63
4.8 Uplift Composite Maps	64
4.9 Chapter Summary	68
CHAPTER 5: FIELD VALIDATION RESULTS	69
5.1 Introduction	69
5.2 Regional Location Map	70
5.3 Kota Belud Field Site (FS1 to FS6)	71
5.3.1 Location Map	71
5.3.2 Kota Belud Field Site 1 (FS1)	72
5.3.3 Kota Belud Field Site 2 (FS2)	73
5.3.4 Kota Belud Field Site 3 (FS3)	74
5.3.5 Kota Belud Field Site 4 (FS4)	75
5.3.6 Kota Belud Field Site 5 (FS5)	76
5.3.7 Kota Belud Field Site 6 (FS6)	77
5.4 Tuaran (Kiulu) Field Site (FS7 to FS11)	78
5.4.1 Overview Map	78
5.4.2 Kiulu Field Site 1 (FS7)	79
5.4.3 Kiulu Field site 2 (FS8)	80
5.4.4 Kiulu Field site 3 (FS9)	81
5.4.5 Kiulu Field site 4 (FS10)	82
5.4.6 Kiulu Field site 5 (FS11)	83
5.5 Kg. Turuntongun Field Site (FS12)	84
5.6 Kundasang Field site (FS13 to FS16)	86

5.6.1	Sg. Mesilau (FS13)	86
5.6.2	Kg. Kauluan (FS14)	88
5.6.3	Sg. Liwagu (FS15)	89
5.6.4	Kg. Kibbas (FS16)	92
5.7	Matopang Field Site (FS17)	95
5.8	Sg. Kagibangan Field Site (FS18)	96
5.9	Chapter Summary	97
CHAPTER 6: DISCUSSIONS, CONCLUSIONS & RECOMMENDATIONS		98
6.1	Introduction	98
6.2	Summary of Results	98
6.3	Discussions	99
6.3.1	Tectonic and Erosion Morphometrics Anomalies in Relation to Faults and Uplift	99
6.3.2	Potential Uplift Sites Based on Morphometrics	101
6.3.3	Field Structures at Uplift Sites	103
6.3.4	Uplift Sites Tectonic Regime and its Implication to Regional Tectonics in NW Sabah	105
6.4	Conclusions	106
6.5	Recommendations	108
REFERENCES		109

LIST OF FIGURES

	Page
Figure 1.1: The topographical map of the major drainage basins that are located on the Kinabalu granite flanks. The active flowing river streams are generated on the respective basin catchment. The darker river lines indicate broader river width and higher volume of stream discharge, while lighter lines reflect tighter and lower stream discharge volume.	5
Figure 1.2: The rock unit distribution of the study area. The thickened black lines represent the known major fault, while the dashed lines reflect the major thrust faults (modified after Tongkul, 2017). The beachballs represent the major and known sources of seismicities based on USGS data.	6
Figure 2.1: Crustal thinning classification of the South China Sea in relation to the NW Borneo, Palawan, and Indochina (Savva et al., 2014).	12
Figure 2.2: The three main rifting phases of the South China Sea in relation to the rift timing (Cullen et al, 2010).	13
Figure 2.3: Seismic expressions of the three main rifting phases and corresponding conceptual models (Franke et al., 2013).	14
Figure 2.4: Structural evolution of South China Sea sea-floor spreading and cessation followed by post-rift magmatism. (Franke et al., 2014)	15
Figure 2.5: The evolution of NW Borneo trough, in relation to the collision of Dangerous grounds. The jammed plate marks the end of the South China Sea rifting (Fyhn et al., 2009)	16
Figure 2.6: The Indian plate collision stages in relation to the left lateral shearing over Indochina, subduction of Proto-South China Sea, and uplift of NW Borneo in the Cenozoic (Hall et al., 2008)	18
Figure 2.7: Reconstructed plate stresses relative to the plate reconfiguration and basin rift. The 5 Ma maximum horizontal stress direction inferred to trend NW-SE (Pubellier & Morley, 2014).	19

Figure 2.8:	The outline of the accreted Rajang-Crocker fold thrust belt during the Cenozoic. (Hall et al., 2008)	20
Figure 2.9:	Tectonic setting of NW Sabah and major outline of active strike-slip systems and active trenches (Tongkul, 2015).	21
Figure 2.10:	The active thrust faults of NW Sabah. The cross-section illustrates the crustal structure of the compression tectonics model of NW Sabah (Tongkul, 2017)	22
Figure 2.11:	The stratigraphic distribution of Cenozoic sediments of the Crocker-Rajang fold thrust belt (modified after Hall & Breitfeld, 2017).	24
Figure 2.12:	Stratigraphy of Crocker-Rajang fold thrust belt relative to respective unconformities (Hall & Breitfeld, 2017).	24
Figure 2.13:	Elevation model of the Kinabalu granite and its respective granitic age units. The inset is an aerial side view of the emplaced pluton (Burton-Johnson <i>et al.</i> , 2017).	25
Figure 2.14:	Cross-section of the Kinabalu granite and the inferred elevation of post-exhumation of the plutonic body (Burton-Johnson <i>et al.</i> , 2017).	26
Figure 2.15:	The tectonic lineament map of the Kinabalu granite illustrating the inferred faults (Cottam et al, 2013).	26
Figure 2.16:	Tectonic setting of the Kinabalu granite within the Crocker fold thrust belt (Wang et al., 2017)	27
Figure 2.17:	Reconstruction of Banda-arc subduction and roll-back at 4 Ma (Hall & Spakman, 2015)	29
Figure 2.18:	Three plausible models of the basement fault continuity within NW Sabah in relation to the active tectonism activity over the Kinabalu granite vicinity (Wang et al., 2017)	29
Figure 2.19:	The compression tectonics suggested by USGS seismicities are mostly concentrated over eastern Sabah along a strike-slip stress boundary (Tongkul, 2017).	31
Figure 2.20:	The normal fault interpreted based on linear features and its corresponding outcropping structures (Tongkul, 2017). The normal fault orients at about N40E.	33

Figure 2.21:	Neotectonism landform over the Meligan-Crocker range. The model illustrates the inferred position of normal and active faults. (Menier et al., 2017)	34
Figure 2.22:	Neotectonic imprint in NW Sabah. The strike-slip movement is identified through the shearing of the coconut trunk. (Tongkul et al., 2017)	34
Figure 3.1:	Research workflow covered in this study. In overall, the workflow is drafted in identifying landform uplift through gradient and erosion anomalies that is later validated and correlated to potential field sites.	36
Figure 3.2:	Digital elevation model sample of Mount St. Helens, Washington (Perez-Pena, 2009) and the compiled TRMM precipitation map of the Eastern Cordillera of the Colombian Andes (Struth et al., 2015).	38
Figure 3.3:	Conceptual model of the Hack's stream-length gradient index and the stream-gradient surface-shape length index.	39
Figure 3.4:	The illustration of the computed chi-factor on each drainage respective of each catchment basin. High values correspond to higher susceptibility to modification and mobility (Willett et al, 2014)	44
Figure 3.5:	Conceptual model of the minimum bulk erosion since the exhumation of the Kinabalu granite.	45
Figure 4.1:	The location of each stream profile for the western and eastern flank water catchments. The lithology of the streams is predominantly sandstone in Tuaran water catchments, while lithologic change was observed over the Kota Belud water catchments.	48
Figure 4.2:	Gradient indices of Western-flank basins, Tuaran (TB) and Kota Belud (KB) water catchment. The overlapping peaks were expressed as overlapping indices highlighting a high-gradient uplift. Significant faults are inferred from the coinciding rapid elevation change and overlapped anomalies.	50
Figure 4.3:	The SL-gradient indices of KSE-KNE water catchment. The overlapping indices is an indicator of high-gradient uplift and faulting. The uplift is characterized as high gradient from the overlapping anomalies and is an indicator in delineating regional faults.	51

- Figure 4.4: The stream-length gradient index (SLGI) extrapolated to show the regional extent of the high anomalies, while the surface-shape length index is overlain over the extrapolated map. There are three major areas identified from the map as high tectonic potential namely the Kinabalu granite, Pinosuk plains, and the Trusmadi range. 53
- Figure 4.5: The local relief anomalies over the studied basins. The knickpoint corresponds to the mapped anomalous change of channel gradient and length. Most of the knickpoints observed does not coincide with the boundaries between the elevated structures and flat plains. Thus, suggesting a very complex landform in delineating uplift. 54
- Figure 4.6: The overview map of 100-m interval knickpoints covering the four major drainage basins. The six zones were delineated based on the site interest and accessibility by major roads. 55
- Figure 4.7: The stream-length gradient index anomaly computed at a 100-m interval; 5-m IFSAR digital surface model for the Kundasang drainage basin knickpoints are compared to the digital terrain model. Regional faulting inferred to trend at N 40 E. 56
- Figure 4.8: The normalized channel steepness index computed for all respective drainage basins. High K_{sn} anomalies observed over several streams, namely the Crocker range, Kinabalu granite, and Trusmadi range. 57
- Figure 4.9: The figure showing high χ values suggested susceptibility to erosional modification. The inset mean precipitation rate suggested that maximum rainfall was observed over highest and lowest elevation. 59
- Figure 4.10: The erodible remnants by precipitation is summarized the M-M' and N-N' transect across the Kinabalu granite. The incision estimates (bottom) for each swath profiles illustrating high incision values predominantly over drastic elevation changes. The incision is computed as the difference between the maximum and minimum elevation. High incision correlates to presence of fault. 60

Figure 4.11:	The map illustrates the basin ridgeline migratory direction predominantly towards northeast in relation to the presently known faults and diffuse boundaries. The figure below shows the inferred extension in relation to the normalized channel steepness index anomaly. Faults are suggested by position of high anomaly.	62
Figure 4.12:	Figure showing the depth of eroded volume. The high erosion depth suggested bulk removal by historical tectonic activity while low erosion depth may correspond to historically low tectonic activity or redeposition.	63
Figure 4.13:	Composite map of stream-length gradient derived knickpoints and indices. The high anomalies over KB-1 is potentially derived from lithologic differences while KSE-3 suggested a presence of a significant fault. The fault trends inferred from the plotted knickpoints suggested to trend at N 40 E.	65
Figure 4.14:	The composite map of eroded depth column suggested a consistent trend of N 40 E (Top). The model suggested characteristics of faulting at the points with rapid changes in erosion depth (Bottom).	66
Figure 4.15:	The NW Sabah 1-km interval knickpoints map. Both stream-length gradient index knickpoints and points of uplift from erosion metrics were overlapped. Field sites of interest were preliminary determined from the working base map.	67
Figure 5.1:	The location of the 18 field sites validated in this study and plotted over the regional field terrain map.	70
Figure 5.2:	The six main field sites validated in Kota Belud. Four field sites were validated at the Wariu river while two sites over at the Kedamaian river. The distribution of shallow earthquake is based on data provided by National Disaster Research Centre (NDRC), UMS.	71
Figure 5.3:	The landform feature of the Kota Belud field site 1 (FS1) suggesting an extensional regime at the stream portion. The accompanying minor strike-slip motion may have diverted the stream direction at the local site.	72
Figure 5.4:	The Kota Belud field site 2 suggested a contiguous intermittent change between rapids and ponding interval from field site 1. The tectonic regime is modelled to be of extensional within this field site.	73

Figure 5.5:	The Kota Belud field site 3 suggested sudden drop in elevation that may be contiguous up to downstream. Thus, the field evidence suggested of an extensional feature.	74
Figure 5.6:	The highest upstream portion of the Wariu river field site validated in this study. The landform consistently suggested of formation due to extensional tectonics.	75
Figure 5.7:	The landform of Kota Belud field site 5 suggested anomalously deep ponding. The formation of the ponding extent may be a result of significant downthrown stream portion.	76
Figure 5.8:	The Kota Belud field site 6 rapids were observed to be both contiguous upstream and downstream. Due to a slower flow rate of the streams, deep ponding was more common throughout the Kedamaian river.	77
Figure 5.9:	The field terrain map of Kiulu river. There are five main sites identified over the Kiulu river. The historical distribution of shallow earthquake data is based on data provided by National Disaster Research Centre, UMS.	78
Figure 5.10:	The field site exhibited multiple intervals of rapids and ponding as a result of extensional tectonics at the field site.	79
Figure 5.11:	The field site suggested potentially significant tectonic activity with the presence of landslide coinciding with the knickpoint.	80
Figure 5.12:	Kiulu river field site 3 validation. The stream exhibit river diversion characteristics and deep ponding over the downthrown block.	81
Figure 5.13:	The stream portion shows contiguous rapids and ponding interval upstream of the Kiulu river. At every point of landform coinciding with the rapids, the stream exhibited slight shifts in river flow direction.	82
Figure 5.14:	A deep ponding observed over the Kiulu Field site 11. This suggested a significant drop in elevation prior to being filled by the flowing stream river.	83

Figure 5.15:	Uplift of alluvial body over at Kg. Turuntongun. The compressional uplift is suggested to be accompanied by a minor strike-slip motion. The uplift trend direction is interpreted to trend at N 40 E.	84
Figure 5.16:	Uplift of alluvial body over at Kg. Turuntongun. The compressional uplift is suggested to be accompanied by a minor strike-slip motion. The uplift trend direction is interpreted to trend at N 40 E.	85
Figure 5.17:	The location of knickpoints over Sg. Mesilau interpreted over 100 m SL-indices. The knickpoints verified are labelled as M2 and M3 respectively and plotted over the Google terrain map.	86
Figure 5.18:	Sg. Mesilau aerial images of the anomaly M2 (A-B) and M3 (C). Anomaly M2 corresponded to a waterfall feature while M3 corresponded to a ponding feature. There were no alluvial preserved upstream as the flow of stream is very rapid.	87
Figure 5.19:	Terrain map of mid-portion, Kundasang section (Kg. Kauluan) with the interpreted knickpoints from 100-m SL-gradient indices over various sources of elevation models.	88
Figure 5.20:	Anomaly K1 suggested a stretch of staircase-like waterfall stream. Adjacent to the stretch, anomaly K2, exhibited ponded boulders feature from an older flooding event. Anomaly K3 suggested ponding feature while anomaly K4 is generated by a man-made feature.	89
Figure 5.21:	Field Terrain Map of the Sg. Liwagu Knickpoint. Cross-section X-X' is approximated to illustrate the structural landform uplift in relation to the knickpoint anomaly. The anomaly is consistent on various sources of elevation models.	90
Figure 5.22:	The figure illustrates aerial image of the Sungai Liwagu knickpoint anomaly. The knickpoint is interpreted to coincided with a previously uplifted landform body that is later incised forming the gorges. The fault and uplift are interpreted to trend at about N 40 E.	91
Figure 5.23:	(A) The field terrain map showing location of knickpoint in relation to the active faulting imprinted over the damaged road. (B) The active fault line also coincided with stream deflection over downstream of Kg. Kibbas. (C) Aerial image of the damaged road. The compression is identified through site visit. The compression trend oriented at N 40 E.	92

Figure 5.24:	Kg. Kibbas knickpoint suggested ponding of boulders with the extent of flooding outlined in the figure. The fault was inferred to trend at N 40 E near a visible landslide. This further consolidated the area as tectonically active.	93
Figure 5.25:	Cross-section X-X' of Kg. Kibbas stream segment in relation to the active fault. The model illustrates the ponding observed over the anticlinal structure in relation to the field evident active tectonics.	94
Figure 5.26:	(A) The terrain map of Matopang field sites. (B-D) The strike-slip feature is suggested by linear features of alluvial while normal faulting is based on deep ponding and staircase stream. (E) The hybrid structural model of a compression-extension uplift.	95
Figure 5.27:	The figure shows the downstream knickpoint of Sg. Kagibangan. The knickpoint coincided with a highly sinuous stream segment. The inferred fault from the uplifted alluvial body suggested compression while the fold limb is suggested to be an older remnant.	96
Figure 6.1:	The figure illustrates the comparison of the KSE-3 sub catchment based on 1 km interval and TB-3 sub-catchment on 100-m interval. The resolution of 1-km interval computation identifies uplift on a regional scale while 100-m interval identifies uplift on a field-scale.	102
Figure 6.2:	The two main tectonic models. The extensional regime exhibits deep ponding due to downthrown blocks while compressional regime suggested alluvial ponding over the incised gorges.	104
Figure 6.3:	The regional cross-section of the study area transecting from the western water catchments to the eastern water catchments. Three models proposed were (1) extensional, (2) compressional, and (3) hybrid.	106

CHAPTER 1

INTRODUCTION

1.1 Research Background

During the past five years, two significant earthquakes of greater than magnitude 5 have occurred in Sabah, both located around the Mount Kinabalu area. The two significant quakes occurred on June 2015 (Tongkul, 2016), while the other as recent as March 2018. The tele-seismic signatures highlighted displacement over the Marakau fault that had generated a 6.0 Ma shallow earthquake in 2015 (Wang *et al.*, 2017). Thus, there is an increased interest over the heavily faulted region of Kinabalu granitoid as the vicinity has been a source of rupture-slippage in the recent shallow quakes (Tongkul, 2017). The deformations in intraplate regions are a consequence of active fault plane displacement that exists due to the accumulated intrinsic stress due to its structural configuration (Bull & Scrutton, 1992). These may occur independently or in absence of a subducting zone (Bracène & de Lamotte, 2002). Hence, to identify potential sites of uplift that has not been known within the intraplate of NW Sabah, the landform will be evaluated using morphometric computation through tectonic and erosional indices (Keller & Rockwell, 1984; Keller & Pinter, 1996).

The uplift can be defined as an elevated landform body where there is an observable disparity in elevation between two adjoined surfaces. These surfaces are usually linked by a steep surface where the faults are located either outcropped or buried. The faults are the plane of displacement that forms to accommodate the plate motions. In this study, we applied several gradient based and erosional morphometric parameters to identify uplift. The gradient has been a crude indicator of uplift for a regionally uplifted body (Davis, 1899) and this may be reflected within the incised stream channels. The gradient can be normalized with a factor to reflect certain attributes namely stream power or as an uplift indicator as applied in many literatures (Chen *et al.*, 2003; Troiani & Della Seta, 2008; Hürtgen *et al.*, 2014; Kothyari, 2015; Pirasteh & Li, 2017; Siddiqui *et al.*, 2017). In many studies, Stream-Length gradient (SL) indices were known to reflect the location of faults in literatures (Jaberi *et al.*, 2018). The SL-indices, however, does not differentiate between a high or low gradient uplift. Thus, a novel formulation, the surface-shape length technique will be applied to supplement the SL-indices in this study.

The NW Sabah is known to have undergone intense uplift and weathering since the Cenozoic (Hall & Nichols, 2002; van Hattum *et al.*, 2006; Morley & Back, 2008; van Hattum *et al.*, 2013). Though climate is known to fluctuate in the Cenozoic, on average, is presumed to be contiguous up to be present day. This is assumed for simplicity as the region is geographically located at the equator since the first rapid uplift during the Cenozoic evolution. However, the climatic forcing imprints are not as conspicuous as imprints by tectonic forcing where the erosional metrics are not directly quantifiable with preserved structures (Whittaker, 2012). Fundamentally, the modern-day landform is a function of tectonic uplift, capacity bedrock erosion and intensity of regional climatic forcing (Ahnert, 1970; Bull, 1991; Whipple & Tucker, 1999; Bull, 2008; Whipple, 2009; Whipple *et al.*, 2013). The drainage stream networks, as a function of climate would modify discharge volume of sediment, hence, reconfiguring patterns of fluvial incision (Sklar & Dietrich, 1998; Wobus *et al.*, 2010; Whitfield & Harvey, 2012). In the earliest works, the slope gradient is directly correlated to the

erosion intensity along a slope (Davis, 1899; Strahler, 1950). Thus, the channel gradient is then integrated as a function of erosion; represented in a normalized channel steepness index where it became an indicator for anomalous erosion streams. On the state of basin-wide scale, the computation of chi-factor elucidates regions susceptible to modification relative to adjacent basins. Therefore, highlighting the phases of basin stage as it shifts towards steady-state from disequilibrium (Montgomery & Foufoula-Georgiou, 1993). The erodible landforms would be highlighted by hypsometry integral (Lifton & Chase, 1992; Ohmori, 1993; Brocklehurst & Whipple, 2004; Whipple, 2004; Pérez-Peña *et al.*, 2009). The future shifts in drainage basins is elucidated with chi-factor to shed light on the present state of erosion within the catchment in NW Sabah. Therefore, the overall interest pertaining to erosion metrics would primarily cover the past, present, and future erosional metrics. However, in terms of uplift, only the past changes through an estimated depth of bulk column will be applied in his study.

In the earliest of days, before the advances of morphometric techniques, the structural characteristics of landform uplift were identified to be associated with some form of ponding or ponded feature (Campbell, 1896). The ponding feature has been a consistent and evident feature for an uplift in many literatures (Hutton *et al.*, 1994; Michetti *et al.*, 2012). For a significant uplift, the knickpoints generally coincide with a waterfall feature (Mathew *et al.*, 2016) or a significant fault scarp (Menier *et al.*, 2017). However, there are several challenges in the identification of structural landforms in NW Borneo. For an intraplate region, the lithosphere motion at a steady state is about 2 mm annually (Gordon, 1995, 1998). Thus, the uplift within NW Sabah is quite miniscule. Previous works on regions with miniscule uplift, suggested an extensive difficulty in identification of any forms of minor uplift (Figueiredo *et al.*, 2018) as it may be potentially obscured (Giamboni *et al.*, 2005). The knickpoints will be validated in the field and it remained an interest to observe the structural landform namely ponding and gorge formation that is pinpointed by morphometrics. Thus, the interest to observe the landform structures as a consequence of uplift in the field of NW Sabah.

1.2 Study Location

The study area within NW Sabah is focused on four drainage streams that surround the Kinabalu granite. Three of the basins with stream source point originating from the highest elevated apex (4095 m), while Tuaran catchment is an independent basin (Fig. 1.1). All the major catchment basins of interest have distinct and unique characteristics. On the western flank, two basins of interest are denoted as the Tuaran basin (TB) and Kota Belud (KB) basin; named respective of their bounded geographical location. The surface of the Tuaran Basin is about 981.92 km², while the Kota Belud basin is at about 859.29 km². On the eastern flank, two catchment basins that drains from the Kinabalu granite is named based on its relative geographical position to the apex, Kinabalu North East (KNE) flank and Kinabalu South East (KSE) flank basin. The KNE catchment basin measures to be about 3113.1 km² of total surface area, while the KSE catchment basin is measured to be about 3529.6 km² of drainage area. Each catchment basin has an active river stream. Tuaran Basin hosts the Tuaran river, while Kota Belud basin hosts the Kedamaian and Wariu river. The length of both streams is approximately 30 km. Sugut river is located in the Kinabalu North-east basin. The Kinabalu South-east (KSE) basin hosts the Labuk river, that were fed by the Liwagu river and Kagibangan river.

1.2.1 Regional Climate

The NW Sabah is classified as an equatorial climate with near maximum humidity, under the Köppen-climate classification (Kottek *et al.*, 2006). The present-day climate of NW Sabah ranged between a low of 24 degrees Celsius to a high of 32 degrees Celsius. However, temperature were significantly lower over highland areas, registering an annual average of 20 degree Celsius. Sabah experiences monsoonal rainfall pattern changes, where the November to December period recorded the wettest season (Chen *et al.*, 2013).

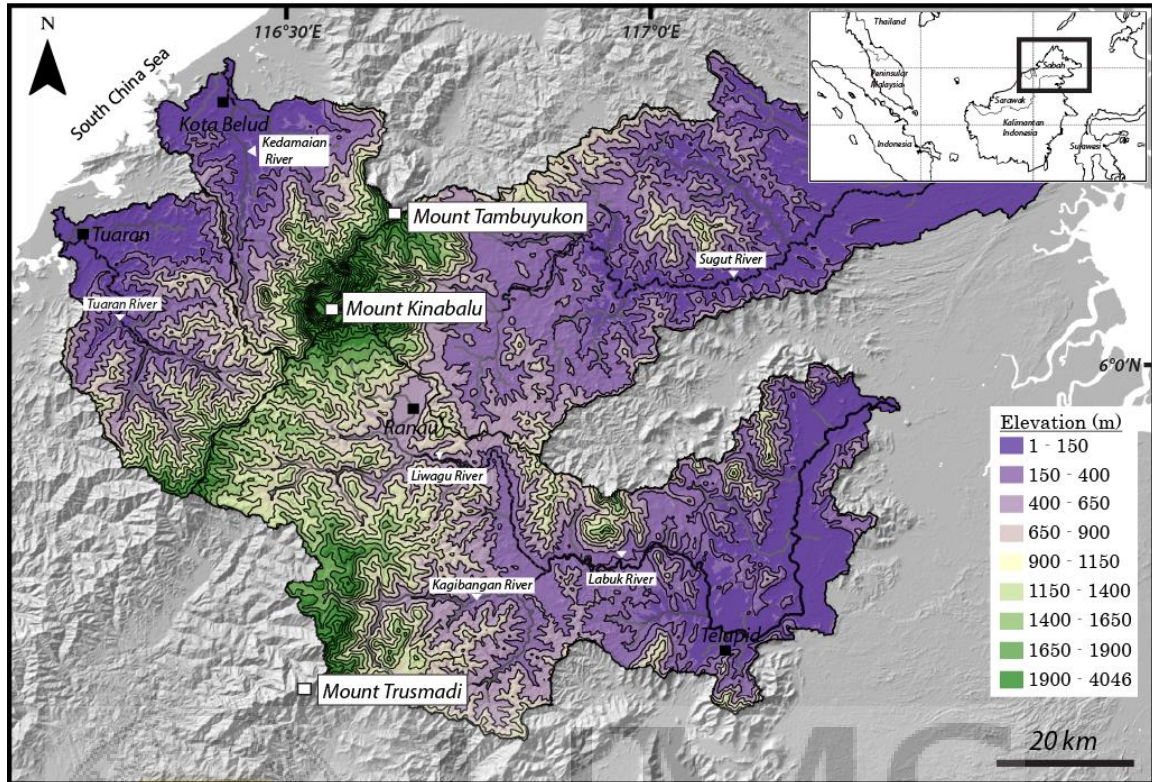


Figure 1.1: The topographical map of the major drainage basins that are located on the Kinabalu granite flanks. The active flowing river streams are generated on the respective basin catchment. The darker river lines indicate broader river width and higher volume of stream discharge, while lighter lines reflect tighter and lower stream discharge volume.

1.2.2 General Geology and Tectonic Setting

The study area is predominantly underlain by a deformed sandstone and shale sequence. The exception is noted for an exhumed granite body with sparsely distributed ophiolitic ultrabasic rocks (Fig. 1.2). This is supported by great number of mapped lithological boundaries in previous literatures (Tongkul, 1993, 1994; Balaguru *et al.*, 2003; Tongkul & Chang, 2003; Balaguru & Nichols, 2004; Hall, 2013; Burton-Johnson *et al.*, 2017). The oldest known formation of Cretaceous-Jurassic origin are the ophiolite outcrops and is regarded as the basement rock in the study area (Tongkul, 1991). A great extent of ophiolitic rocks within the study area were observed